Basic features of boron isotope separation by SILARC method in the two-step iterative static model

K. A. Lyakhov · H. J. Lee

Abstract In this paper we develop a new static model for boron isotope separation by the laser assisted retardation of condensation method (SILARC) on the basis of model proposed by Jeff Eerkens. Our model is thought to be adequate to so-called two-step iterative scheme for isotope separation. This rather simple model helps to understand combined action on boron separation by SILARC method of all important parameters and relations between them. These parameters include carrier gas, molar fraction of BCl_3 molecules in carrier gas, laser pulse intensity, gas pulse duration, gas pressure and temperature in reservoir and irradiation cells, optimal irradiation cell and skimmer chamber volumes, and optimal nozzle throughput. A method for finding optimal values of these parameters based on some objective function global minimum search was suggested. It turns out that minimum of this objective function is directly related to the minimum of total energy consumed, and total setup volume. Relations between nozzle throat area, IC volume, laser intensity, number of nozzles, number of vacuum pumps, and required isotope production rate were derived. Two types of industrial scale irradiation cells are compared. The first one has one large throughput slit nozzle, while the second one has numerous small nozzles arranged in parallel arrays for better overlap with laser beam. It is shown that the last one outperforms the former one significantly. It is argued that NO_2 is the best carrier gas for boron isotope separation from the point

of view of energy efficiency and *Ar* from the point of view of setup compactness.

1 Introduction

Boron isotopes have a broad spectrum of applications in industry. Naturally occurring boron consists of two stable isotopes—19.9 % of boron-10 and 81.1 % of boron-11. A useful property of pure boron-10 isotopes as large thermal neutron absorption cross-section makes separation of isotopes highly desirable. In nuclear plants, for instance, boron-10 saturated compounds are used as control rods and as reactor coolant additives due to their large thermal neutron absorption cross-section (3837 barn for boron-10 and 0.005 barn for boron-11). Increased boron-10 to boron-11 ratio in the boric acid solution, used as a chemical shim in Pressurized Water Reactors (PWR), allows to reduce the total amount of boron-based poison material in the primary reactor coolant system, and, therefore to reduce corrosion and wear on the other components of the reactor core [1]. boron-10 saturated compounds are also used in nuclear reactors emergency shutdown systems. Boron is routinely used in microelectronics for producing p-type domains in silica. Use of isotopically pure boron minimizes the thickness of boron acceptor layers, increases the heat conductivity of the acceptor layer and increases the transistor switching power [2]. In spacecraft semiconductors boron-10 enriched materials are used for radiation shielding, while boron-11 can be used in semiconductors when protection from cosmic and other kinds of radiation is important. This protection is getting more important with advancing miniaturization of electronic devices, and in helioenergetics [3, 4]. In nuclear medicine boron-10 is used in so-called boron neutron capture cancer therapy [5].

K. A. Lyakhov · H. J. Lee (✉)
Plasma Physics Laboratory, Department of Nuclear and Energy Engineering, Applied Radiological Science Research Institute, Jeju National University, Ara-dong 1, Jeju 690-756, South Korea
e-mail: hjlee@jejunu.ac.kr

K. A. Lyakhov
e-mail: lyakhov2000@yahoo.com

There are a number of laser assisted methods: molecular obliteration laser induced isotope separation (MOLIS), chemical reaction by isotope selective laser activation (CRISLA), separation of Isotopes by laser assisted retardation of condensation (SILARC) (in [6] it is also called as CRISLA-1), condensation repression by isotope selective laser activation cold walls harvesting scheme (in [6] this scheme is abbreviated as CRISLA-2), and atomic vapor laser isotope separation (AVLIS). All these methods are based on selective laser energy delivery to target isotopes. Selectivity is provided by sharp photon energy dependence of the photoabsorption cross section, that is specific for different isotopes.

In MOLIS scheme clusters are formed via recombination of selectively dissociated BCl_3 molecule with a scavenger gas. Apparently energy expenses for MOLIS are more significant since it is necessary to break strong intermolecular bonds to form new clusters selectively. According to [7], in order to prevent target molecule dissociation, this molecule should have been transferred, the energy of at least one IR photon energy in excess to its binding energy (this is so-called molecule dissociation threshold). For instance in order to compare, decomposition of $BCl_3:NO_2$ dimer (corresponding van der Waals binding energy is $U_{vdW} = 510\,cm^{-1}$ [8]) or to prevent dimerization (as shown in [9] these processes are physically equivalent) requires only one $\alpha = v_3$ vibrational mode ir-photon energy, while BCl_3 molecule dissociation(corresponding binding energy is $D_\alpha = 38,000\,cm^{-1}$ [10, 11]) requires absorption of at least 39 ir-photons. This suggests a rather large laser energy pumping speed in the medium when using the MOLIS scheme.

In the CRISLA harvesting approach energy expenses are also substantial. These energy expenses include energy of vibrational activation of the target isotope to enhance the reaction rate through a specific co-reactant added to the BCl_3+CG mixture (CG denotes carrier gas), and energy needed for molecular rearrangements in the newly formed dimer [12]. These two schemes both require either multiphoton or UV photon+IR photons absorption. Moreover, formidable side reaction problem arises in that the enriched products, that are formed in the gas phase, tend to form product depleted heteroclusters in supercooled conditions.

In the AVLIS scheme energy expenses are even more higher. They include energy spent for the laser pumping system, and energy consumed by vaporizer/separator plus isotope ionization energy [2].

Our choice of SILARC as an objective for current study is motivated by its relatively high selectivity and substantially lower energy consumption. Viability of this scheme for SF_6 isotope separation was confirmed experimentally in [13, 14]. This separation approach is based upon selective excitation of target isotopes in an overcooled gas flow by a specifically tuned laser frequency. Overcooled gas flow can be produced either by Laval nozzle or by orifice plate. In order to gain better gas flow and laser beam overlap gas pulse repetition rate should be synchronized with a sequence of laser pulses. The separation principle is based upon selective condensation of dimers that are mainly composed of unexcited isotope molecules and carrier gas molecules [6]. Another one is based on the concentration of heavier dimers that has a smaller diffusion rate compared to the excited isotopic molecules in the jet core region. Boron isotope separation in SILARC can be schematically represented as: At $T > T_c$: $BCl_3 + CG \rightarrow BCl_3 : CG \rightarrow BCl_3 + CG$, where BCl_3:CG denotes dimer, T_c is gas condensation temperature. At $T < T_c$:$^{10}BCl_3 + CG + hv \rightarrow {}^{10}BCl_3^* : CG \rightarrow {}^{10}BCl_3 + CG + \Delta E, {}^{11}BCl_3 + CG \rightarrow {}^{11}BCl_3 : CG + {}^{11}BCl_3 : CG : open\ surface$. Gas expansion from the reservoir chamber to the inlets of vacuum pumps in this scheme can be described by hydrodynamic equations with an ideal gas equation of state, where selective dimerization in a laser field is treated within the transport equations framework, as shown in [8, 17]. In this paper we found the most optimal carrier gas from N_2, Ar, NO_2, and SF_6 carrier gases.

Boron isotope enrichment factor has an essential dependence on the laser intensity. The higher laser intensity is the larger enrichment factor, that saturates, however, rapidly after some limit as will be shown later. Moreover, if laser fluence is high enough, caution must be exercised because multiphoton absorption can take place [7]. In this case applying of static approach is questionable. However, laser pulses of rather small intensities or continuous wave mode can be as much effective as sequence of laser pulses of high intensity. In this case weakness of interaction with laser field is compensated by longer interaction time that leads, according to definition of excitation rate given in [17], to the same probability of selective excitation as for pulsed mode. IC is designed as a multi-pass cavity, discussed in this paper, can significantly extend reaction volume, and therefore significantly reduce laser energy needed. In such IC, the walls that are placed cross-wise to laser beam and along the gas flow can be polished for high reflectivity.

In the CRISLA-2 scheme, gas flow is irradiated coaxially to the IC axis. This is conditioned by cylindrical geometry of IC most suitable for selective condensation of target isotopes on its walls employed in this method [6].

Another important aspect is selectivity. It can be quantitatively estimated by widening of photoabsorption spectral lines, basically caused by thermal (Doppler) and pressure (collisional) broadening. For CRISLA-2 power broadening is negligible due to rather small laser intensity

required. Doppler and collisional broadening can be reduced by letting the gas to supersonically expand through Laval nozzle. However, as shown in [17], gas cooling below some temperature is not desirable because product cut from selective excitation of isotopes, residing mainly in dimers, is very small. Furthermore, collisional broadening can be reduced either by diminishing nozzle throughput or by increasing pumping speed in order to reduce gas density in IC. However, for our case of interest—boron isotope separation, broadening effects are rather small compared to large isotopic shift $\sim 39\,\mathrm{cm}^{-1}$ [15]. Indeed, for instance, Dopplers shift at optimal temperature for NO_2 used as a carrier gas ~ 80 K, is very small $\Delta\nu_D \sim 10^{-2}\,\mathrm{cm}^{-1}$. In SILARC-2 scheme, in order to gain better selectivity, target molecules have to be substantially diluted in carrier gas, so that laser excitation of one isotope in the collisional region of the free jet expansion is not followed by significant, nearly resonant, intermolecular vibrational energy transfer [9].

As shown in [8] on example of UF_6 dissolved in nitrogen, clusters of critical size in SILARC scheme conditions form at some time after the boiling temperature of gas mixture is achieved. However, if the overcooling time is larger than critical size cluster formation time, then irreversible cluster growth takes place. It is rather undesirable because clusters are normally ionized in external electromagnetic field but not decouple [18]. For IC length $L_{IC} \sim 50 \div 70$ cm, the transition time of molecules across IC (residence time) is quite short compared to critical size cluster formation time. However, residence time can become much longer if gas evacuation rate is not high enough. Another side effect of too long residence time is that pressure and temperature growth in IC will also deteriorate selectivity. Then in order to dilute gas, provided pumping down rate stays the same, a combination of harvesting methods can be useful. For instance, as pointed out in [17] dimers can be deposited on zigzag or wavy plates or scrubbers that can be placed just before skimmer blade.

To summarize, optimal gas pressure in IC can be provided by appropriate nozzle throat area, number of nozzles, IC volume, valve opening time, and gas evacuation rate. Enrichment factor depends on efficiency of the harvesting scheme, which is directly related to the laser intensity, gas evacuation rate, and skimmer placement. Obviously, the correct answer for the question which enrichment facility design is most effective should be a compromise between selectivity, energy expenses, performance and the total volume of the system. As shown in this paper all these parameters are interrelated, and they should provide global minimum of total energy expenses in order to achieve desired production rate.

2 Irradiation conditions

In this section, we introduce major parameters attributed to laser field influence on effectiveness of enrichment. According to experimental data from [19], near resonant cross section of BCl_3, corresponding to $\nu_3 = 997\,\mathrm{cm}^{-1}$ vibrational mode, [15], is rather small: $\sigma_A = 7.1 \times 10^{-20}\,\mathrm{cm}^2$. This suggests using a rather large laser intensity to provide larger laser excitation rate, and, therefore, larger enrichment factor in accordance with its definition given in [17]. Laser excitation rate of molecules by selective photoabsorption is given by:

$$k_A = \phi_L \sigma_A, s^{-1} \text{ per molecule,} \tag{1}$$

where photon flux is:

$$\phi_L = \frac{5.035 \times 10^{22} I_L(\mathrm{W/cm^2})}{\epsilon_3(\mathrm{cm}^{-1})}, \text{ photons} \times \mathrm{cm}^{-2}\,\mathrm{s}^{-1}, \tag{2}$$

where laser photon energy $\epsilon_3 = h\nu_3$ corresponds to ν_3 mode of $^{10}BCl_3$ absorption band. Due to a very small frequency shift, the same photon energy can be used for selective dimer excitation. However, dimer photoabsorption cross section is about 10 times smaller than that of monomers [17]. Then an early start for the gas flow cross-wise irradiation, when the monomer fraction is still large, is preferable. Laser beam energy density is $I_L = I_0/(\pi R^2)$, where R is laser beam radius. Effective laser pulse intensity can be introduced as

$$I_0 = \kappa I_P. \tag{3}$$

Under term "effective laser pulse intensity" we assume that only a fraction of overall gas expansion time gas flow is affected by laser field. This fraction is directly related with reaction volume V_{int} by the factor κ

$$\kappa = \frac{t_{int}}{t} = \frac{V_{int}}{V}, \tag{4}$$

where $V_{int} = A_f L_{int}$ is the volume of overlap region between laser beam and gas flow, $V = A_f L$ is the gas flow volume, A_f is the cross-sectional area of gas flow, L is the gas flow length, and $L_{int} = U_s t_{int}$ is the overlap region length. In cross-wise gas flow irradiation overlap region length can be introduced as

$$L_{int} = N_{tr} l, \tag{5}$$

where N_{tr} is the number of laser beam and gas flow intersections. For laser beam and gas flow, intersecting under angle α, intercept length apparently is $l = \frac{2R}{\sin\alpha}$. The number of laser beam passes across the gas flow (laser beam radius is R) is given by

$$N_{tr} = \frac{L}{H \tan \alpha + l}, \tag{6}$$

where H is IC height. Therefore the factor κ is given by

$$\kappa = \frac{l}{l + H \tan \alpha}. \tag{7}$$

Apparently, in order to use laser energy more efficiently number of intersections should be made as large as possible. The relation between acceptable laser energy loss $\kappa = \kappa_0$, laser intensity per pulse I_P, IC geometry, and angle α follows from Eq. (7):

$$\sin \alpha = \left(\frac{1}{\kappa_0} - 1 \right) \frac{2R}{H}. \tag{8}$$

3 The static model for two-step iterative scheme of isotopes enrichment

The answers for questions, which carrier gas is most optimal, which gas flow pressure and temperature are optimal, and what is the optimal IC volume to gain necessary production rate by enrichment setup, can be given on the basis of the model developed in [8, 17]. This model can be described as a material and kinetic balance equations approach for four (three for dimers excitation) fractional population groups for target isotopes in a selectively acting laser field. These groups include $^{10}BCl_3^*$ excited, $^{10}BCl_3$ non-excited monomers, $(^{10}BCl_3)_i$ epithermals, and $^{10}BCl_3$: CG dimers, or the same groups except excited monomers for dimer excitation case. After isotope-selective excitation of $^{10}BCl_3$ the $^{10}BCl_3^*$ will dimerize briefly as $^{10}BCl_3^*$: CG, that rapidly dissociate with VT conversion, creating epithermals. Boron-11 isotopes are distributed over the groups of thermal monomers and slower moving dimers. To reduce resonant photon exchange probability between already selectively excited isotopes, these isotopes should be strongly diluted in carrier gas. In our calculations we used the value from [16] for the optimal molar fraction of SF_6 or UF_6 molecules dissolved in N_2 carrier gas, that is $\mu = 0.02$. This value can be decreased even more in order to increase enrichment factor, but at the same time it will also induce undesirable product cut reduction.

Fig. 1 **a** Enrichment factor as a function of temperature at different laser pulse intensities. BCl_3 is mixed in NO_2 with molar fraction $\mu = 0.02$. Nozzle orifice area, IC and skimmer chamber lengths, and valve opening time correspond to local minimum evaluated by routine 'NLPSolve' from Optimization Toolbox of Maple15 [23]. Values of these parameters are gathered in Table 1 in the Sect. 6. Sequence of laser intensities was chosen for best resolution of curves. **b** Product cut for the same parameter set
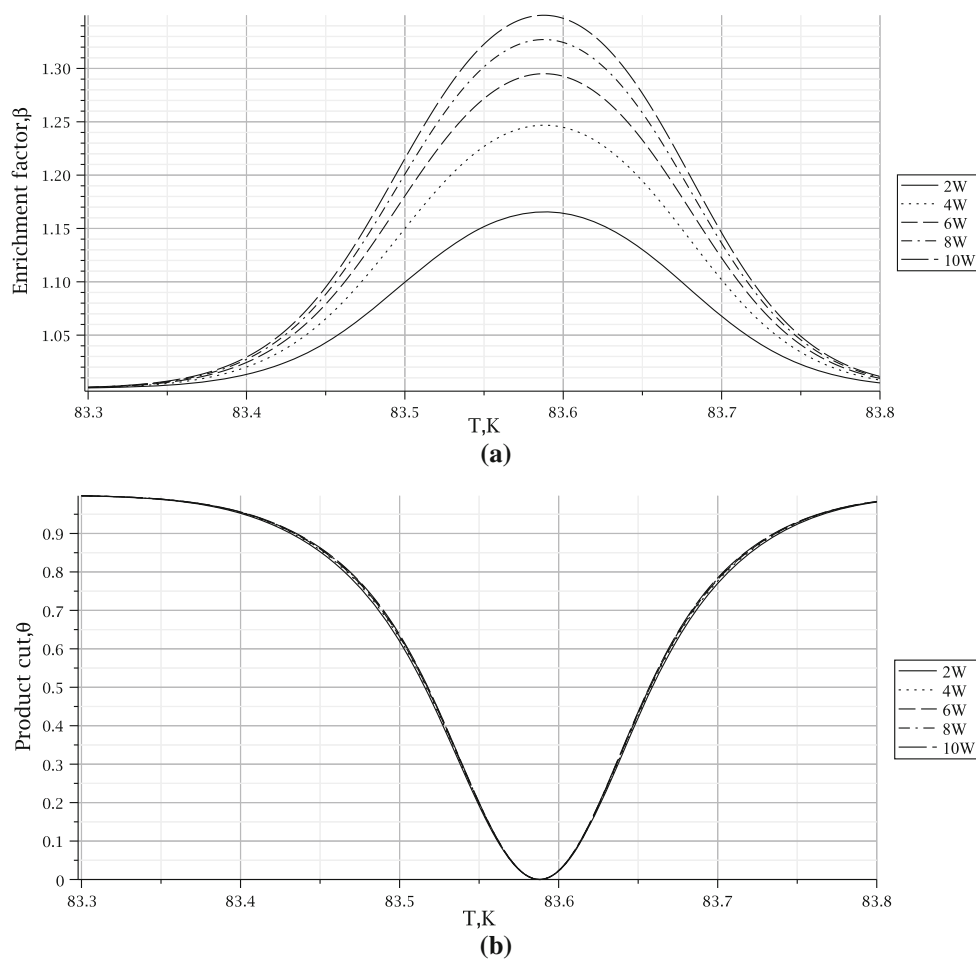
We assume that laser fields are relatively weak. As shown later they are produced as a sequence of pulses of rather long duration (>1 ns). In this case time dependence of the field amplitude does not play an essential role [20]. Gas flow is also assumed steady so that pressure in feed chamber evolves as a step-like function (it remains constant over all the time period, when valve is open). Then the system of transport equations derived in [17] reduces to the system of algebraic equations. By solving these equations one can find enrichment factor β and product cut θ for given carrier gas, nozzle throat area, IC length, skimmer location, gas/laser pulse duration and periodicity, temperature and pressure inside the gas flow. At calculation of these quantities we consider only monomer excitation.

In Fig. 1 it is seen that increasing laser intensity increases enrichment factor up to some limit but practically does not affect product cut. This saturation is of course explained by normalization condition for laser-pumped excited fraction of isotopes. The first thing that is seen is that all curves for product cut practically coincide. According to the definition of product cut given in [17] it is practically unaffected by intensity of laser radiation provided boron-10 isotope abundance is $x_i \ll 1$. This isotope abundance is introduced as

$$x_i = \frac{n_i}{n_Q} \equiv \frac{[^{10}\text{BCl}_3]}{[^{11}\text{BCl}_3] + [^{10}\text{BCl}_3]}. \tag{9}$$

The second remarkable feature is that it gets almost zero at some critical temperature. This minimum is explained by strong dependence of product cut on nozzle throat area. Namely, the larger the nozzle throat area the smaller is the product cut. The same result follows as well from behavior of recycling factor as a function of nozzle throat area, that is discussed in the Section 5. At the critical temperature, that can be derived from its definition, Eq. (35), factor x becomes singular. The factor x is related to the nozzle throat

area as $A_t = xD^2$. This factor behavior in the close vicinity of critical temperature is displayed below in Fig. 2. At $T < T_c$, it gets negative, and, therefore, leads to negative sign of nozzle throat cross section. Thus, it is just an artefact of our model. We found that the same situation takes place, but for different critical temperatures, for all other carrier gases considered—N_2, Ar, SF_6.

We assume that gas flow pressure in two downstream chambers, IC and skimmer chamber, evolves as a two-stage process. In the first stage gas expands into IC through the nozzle throat while control valve is open. Gas influx leads to pressure build up in IC and skimmer chamber from the initial one P_{in} to the final one P_{fin}, so that pressure varies inside interval $P_{in} - P_{fin} = \Delta P$ around $\bar{P} = 0.01$ torr. This variation should be small enough in order to preserve selectivity and minimize collisional excitation loss (in calculations we assume $\Delta P = 0.01$ torr). This stage occupies the time interval equal to gas pulse duration $\tau_p = \frac{\Delta P}{A}$. Parameter A is related to pressure increment in IC produced by collective throughput Q from all nozzles that can be calculated by Eq. (16),

$$\Delta P = k_B T_0 \Delta C, \quad \Delta C = Q \frac{\tau_p}{V_1(1+\Gamma)} \Rightarrow A$$
$$= k_B T_0 \frac{Q}{V_1(1+\Gamma)}. \tag{10}$$

Thus the pressure increment reads

$$\Delta P = Q\tau_p \frac{k_B T_0}{V_1 + V_2}. \tag{11}$$

The second step corresponds to gas evacuation stage from P_{fin} to P_{in}. Duration of this step can be estimated as

$$t_{out} = g_0 \rho (V_1 + V_2), \quad \rho = \frac{\ln\left(\frac{P_{in}}{P_{fin}}\right)}{N_{in}} \left(\frac{dU_A}{dt}\right)^{-1}, \tag{12}$$

where V_1 is the IC volume, V_2 is the skimmer section volume, N_{in} is the number of vacuum pumps, and dU_A/dt is

Fig. 2 Factor x as a function of temperature (**a**) on the left-hand side, and (**b**) on the right-hand side from its singularity, corresponding to the critical temperature $T_c = 83.588$ K, provided NO_2 is used as a carrier gas. Parameter set is fixed to the values gathered in Table 1
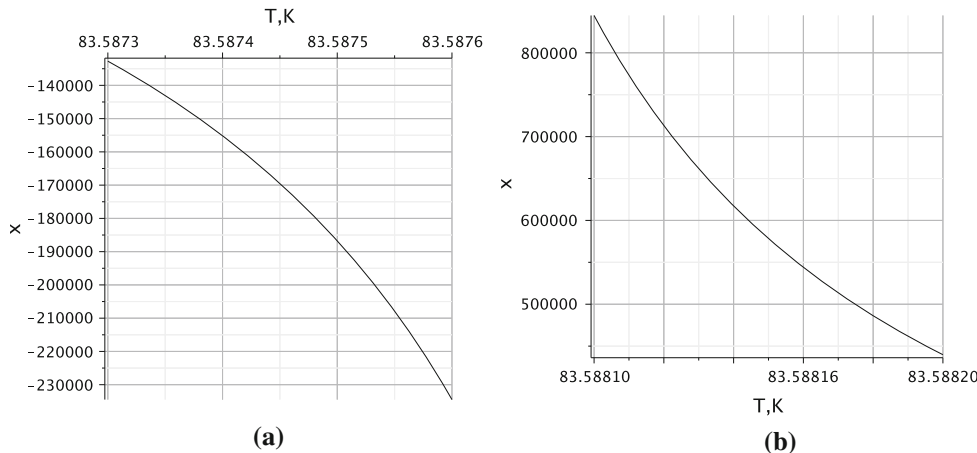
the performance of each vacuum pump, factor g_0 takes into account outgassing that is important in the pressure range operated $P_{\text{fin}} \geq P \leq P_{\text{in}}$ [24]. Volume of skimmer chamber is introduced as $V_2 = \Gamma V_1$, where value of parameter Γ is defined by optimization procedure described in the last section. Gas evacuation time is much longer than thermal equilibrium time between these chambers and their walls. This explains our assumption that pressure and temperature in both chambers are the same. Shortly afterwards gas is equilibrated with walls that are maintained at room temperature T_0.

Gas flow rate across orifice between reservoir with initial gas pressure P_0 and downstream chamber with initial gas pressure $P_{\text{in}} = \bar{P}$ for isentropic gas expansion can be estimated as

$$Q = N_{\text{nozz}} C_f A_t S, \quad S = \sqrt{\frac{P_0 n_0}{m_0} \frac{2\gamma}{\gamma - 1} \left[\left(\frac{\bar{P}}{P_0} \right)^{\frac{2}{\gamma}} - \left(\frac{\bar{P}}{P_0} \right)^{\frac{\gamma+1}{\gamma}} \right]},$$

$$n_0 = \frac{P_0}{k_B T_0}, \tag{13}$$

where N_{nozz} is the number of nozzles and m_0 is the molar mass of gas mixture used. Specific heat ratio for gas mixture is given by

$$\gamma = \frac{(1 - \mu)C_p^G + \mu C_p^Q}{(1 - \mu)C_v^G + \mu C_v^Q}, \tag{14}$$

where μ is the molar fraction of BCl_3 in carrier gas, and $C_p^{Q,G}, C_v^{Q,G}$ are specific heats at constant pressure and volume, respectively, for corresponding gas fractions. Flow

Fig. 3 **a** Factor x, **b** enrichment factor, and **c** product cut as functions of temperature for different carrier gases. Corresponding optimal parameters are gathered in Tables 1 and 2

(a)

(b)

(c)
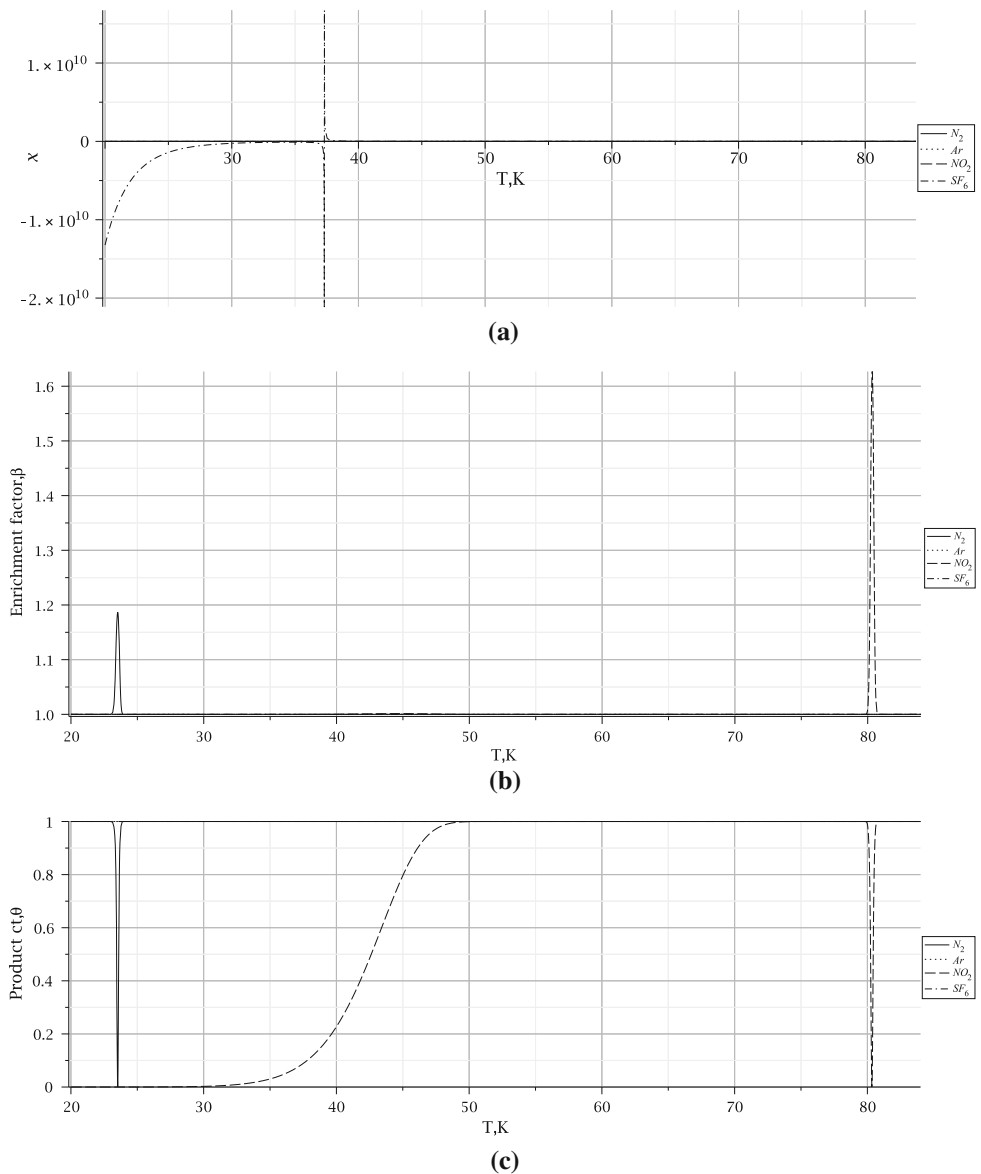
coefficient C_f depends on the boundary layer width. Nozzle throat area is $A_t = DH$, where D, H are nozzle height and width, respectively. In the formula (16) initial pressure in reservoir is not known. It can be found from relation between upstream and downstream pressure and temperature for one-dimensional isentropic gas expansion:

$$\frac{T}{T_0} = \left(\frac{\bar{P}}{P_0}\right)^{\frac{\gamma-1}{\gamma}}. \tag{15}$$

The initial value of gas pressure in downstream chamber should be chosen to provide required gas cooling, and, at the same time, to minimize gas flow overexpansion, which takes place when initial pressure in IC is significantly smaller than pressure at the nozzle outlet [21]. Downstream gas flow optimal temperature is assumed corresponding to the minimal value of objective function introduced in the last section, Eq. (40). However, until now we were able to find a only a local minimum by using nonlinear programming routine 'NLPSolve' from Optimization Toolbox of Maple15 [23]. Our calculations for enrichment factor and product cut as a function of temperature are shown in Fig. 3.

The largest value of enrichment factor for NO_2, used as a carrier gas, can be explained by that, in addition to conclusion made in [17] about influence of carrier gas molecular mass on enrichment factor, it also depends strongly on hetero-dimer binding energy. Indeed, enrichment factor depends mostly on the availability of monomers at lower temperatures and dimer decay rate at higher temperatures. According enrichment factor asymptotic at $x_i \ll 1$, evaluated in [17], if dimer decay rate is small, but nevertheless temperature is large enough for sufficient monomer availability, it can be increased by increasing binding energy that corresponds to decreasing dimer decay rate. We estimate binding energy of BCl_3 with carrier gas (CG) as $D(CG:BCl_3) = \sqrt{D_\alpha(BCl_3)D_\beta(CG)}$, where $D_\alpha(BCl_3) = 104 \, \text{cm}^{-1}$ is the binding energy of dimer formed from two BCl_3 molecules (monomers). According to calculations based on the dimerization model proposed in [8], NO_2 has the largest binding energy among other considered carrier gases: $D_\alpha(NO_2) = 2{,}500 \, \text{cm}^{-1}$.

Gas flow rate across orifice between feed chamber with gas pressure P_0 and IC with initial gas pressure $P_{in} = \bar{P}$ for isentropic expansion case can be estimated by

$$Q = N_{nozz}A_t S, \quad S = C_f\sqrt{\frac{P_0 n_0}{m_0}\frac{2\gamma}{\gamma-1}\left[\left(\frac{\bar{P}}{P_0}\right)^{\frac{2}{\gamma}} - \left(\frac{\bar{P}}{P_0}\right)^{\frac{\gamma+1}{\gamma}}\right]},$$
$$n_0 = \frac{P_0}{k_B T_0}, \tag{16}$$

where N_{nozz} is the number of nozzles. Flow coefficient C_f depends on the boundary layer, that is effectively reducing

orifice area. Nozzle throat area is $A_t = DH$, where D, H are nozzle height and width, respectively.

4 Basic operational principles

After finishing two-step process described above, product enriched gas component reiterates back to the feed chamber, where it mixes with new and leftover portions of gas in the chamber, so that reservoir pressure returns to its original level. This procedure goes on until isotope content in reservoir chamber achieves required enrichment level. This level(degree) can be introduced as selected isotopomer and isotopomer mixture ratio of concentrations by the end of enrichment operation $t = t_f$:

$$c_0 = \frac{n_i(t_f)}{n(t_f)}. \tag{17}$$

Therefore, according to definition of factor x_i given by Eq. (9), it is related with c_0 as

$$c_0 = x_i(t_f = nt_c), \tag{18}$$

provided it remains constant on each enrichment iteration (in our calculations we assume that $c_0 = 0.9$). Therefore corresponding number of recyclings is given by

$$n = \log_\beta\left(\frac{c_0}{x_i}\right). \tag{19}$$

Time interval of one enrichment cycle can be introduced as

$$t_c = \tau_L + t_{out}, \tag{20}$$

where $\tau_L = \tau_p + t_{tr}$ is laser pulse duration. Gas flow transition time across IC is given by $t_{tr} = L/U_s$, where U_s is gas flow average velocity

$$U_s = U_{s0}\left[\sqrt{\frac{2}{\gamma-1}\left(1 - T/T_0\right)} + \sqrt{\frac{2}{\gamma+1}}\right]/2,$$
$$U_{s0} = 9116.5\sqrt{\gamma T_0/M \, (\text{amu})}, \quad \text{cm/s} \tag{21}$$

with M being atomic mass of the gas molecules in amu, and T_0 gas temperature in reservoir conditions.

In some sense such recycling loop system can be thought as an open system with positive feedback. We call it as open system because it is connected to mixing tank via negative feedback, responsible for reservoir pressure restoration until predefined initial level.

Let us consider this recycling process in more detail. We assume that there are N_0 molecules in reservoir. This number is conserved because of admixing with fresh portions of gas before start of new iteration as described earlier. Then after the first stage the following equality is valid

$$N_0 = x_i\mu\beta\theta N_0 + N_1, \qquad N_1 = N_0(1 - x_i\mu\beta\theta). \tag{22}$$

Then on the second stage we have

$$N_0 = x_i\mu\beta\theta N_0(1 - x_i\mu\beta\theta + \beta\theta) + N_2,$$
$$N_2 = N_0[1 - x_i\mu\beta\theta(1 - x_i\mu\beta\theta + \beta\theta)], \quad (23)$$

and so on until the necessary level of enrichment is reached. This process requires n recyclings. The number of isotopes, that are collected in reservoir on the last iteration, can be deduced by induction from the previous formulas

$$N_n = N_0\aleph, \qquad \aleph = \frac{x_i\mu}{1 - x_i\mu}\frac{z - z^n}{1 - z}, \qquad z = \beta\theta(1 - x_i\mu),$$
$$(24)$$

where factor $\aleph$ we will call as a recycling factor.

5 Comparison between single and multi-nozzle industrial enrichment setups

In this section, we introduce two types of industrial scale enrichment schemes. In the first one gas expands across a large throughput slit nozzle (Fig. 4a). In the second one it is divided among a collection of parallel to each other rows of slit nozzles (Fig. 4b). Laser beam impinges gas flows produced by nozzles from the same row many times cross-wise as shown in the schemes below. For effective use of laser energy, gas flow should be irradiated in multi-pass cavity. For instance advantages of Herriott cavity or LMPC can be taken in order to provide larger irradiation volume [22].In what follows we demonstrate that performance of one nozzle gets smaller with increasing throat area. According to formulas (16, 24), recycling factor should be used to show this. We calculated this factor as a function of throat height D for different carrier gases. This function is displayed in Fig. 5. Corresponding set of parameters was found by applying nonlinear programming routine 'NLPSolve' from Maple15 [23], for minimization of objective function introduced in the last section, Eq. (40). This result suggests that application in industry of one large throughput nozzle is meaningless.

Fig. 4 a Industrial scale IC with single nozzle. **b** Multi-nozzle industrial scale IC
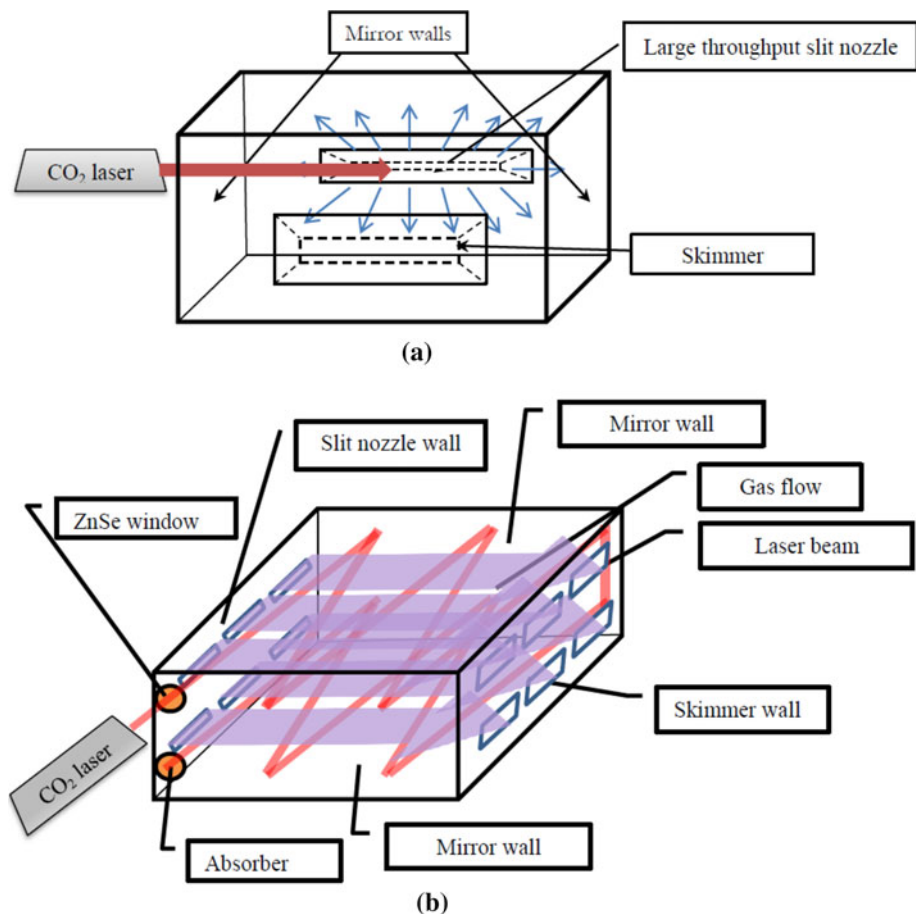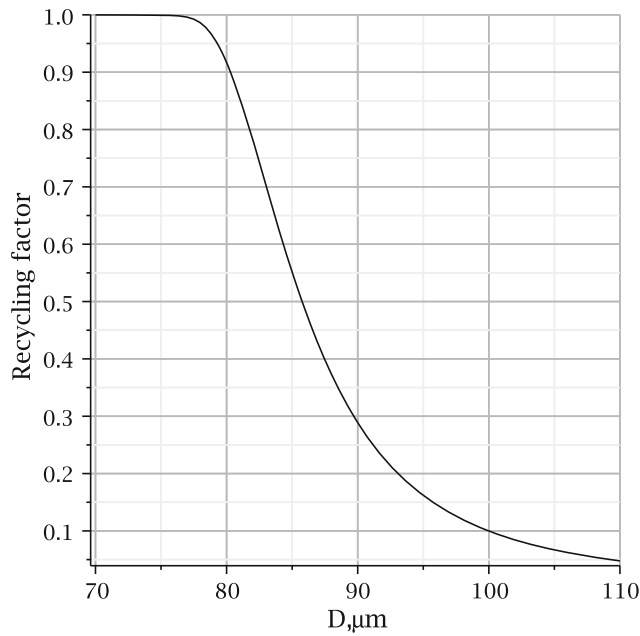
Fig. 5 Recycling factor ℵ as a function of nozzle throat height D for NO_2 used as a carrier gas. Corresponding optimal values of parameters are gathered in Table 1

6 Irradiation cell volume

In this section we present a method to calculate IC volume, which meets requirements of production rate and corresponds to minimum of spent energy

$$E_{tot} = (N_{in}E_W t_{out} + I_P \tau_L / \eta) mn, \quad (25)$$

where N_{in} is the number of vacuum pumps and η is the CO_2 laser efficiency (we assume that $\eta = 0.1$). Vacuum pump motor rating can be estimated by formula from [24]

$$E_W = \frac{dU_A}{dt}(P_{in} - P_{fin})\eta_{mech}^{-1}. \quad (26)$$

In the pressure diapason operated, Roots blower is more appropriate. As illustrated in our calculations we take its pumping speed to be $\frac{dU_A}{dt} = 5,000 l/s$ that corresponds to 'Okta 18000' model issued by Pfeiffer Vacuum. Mechanical efficiency of Roots pump is $\eta_{mech} = 0.85$.

Minimum of energy expenses can be provided by shortening gas residence time in downstream chambers, that is equivalent, according to Eq. (12), to reducing their volume. This volume, as shown later, depends on carrier gas choice, valve opening time, laser pulse intensity, nozzle throat dimensions, IC and skimmer chamber volumes, distance between skimmer holes (factor r in Eq. (31)), temperature and pressure inside the gas flow, and number of vacuum pumps.

As far as it was demonstrated in the previous section, using of multi-nozzle IC is significantly more

advantageous, we assume that gas flow is divided by nozzle wall into set of sub-flows so that dimers, that are formed gradually from molecules unaffected by laser irradiation, from one nozzle do not interfere with dimers from neighbor nozzles. In another words bunch of dimer trajectories, that belong to sub-flow from one nozzle are assumed as confined within the same elementary volume, or cell, along its travel path. Apparently length of this volume corresponds to IC length and its cross-sectional area should be larger than the area of skimmer hole, because its central part is occupied by gas flow core and remaining part should be sufficient to minimize interference between subflows from neighbor nozzles. We assume that skimmer hole, corresponding to slit nozzle, is rectangular. Thus IC volume can be calculated by

$$V_1 = N_{nozz}v_{cell}, \; v_{cell} = D'H'L_{IC}, \; D' = \omega D + 2\delta, \\ H' = H + 2\delta, \quad (27)$$

where L_{IC} is the IC length. Factor ω takes into account nozzle shape geometry. This value is nothing but the ratio of nozzle outlet area to the nozzle throat area

$$\omega = \frac{A_e}{A_t}. \quad (28)$$

This ratio can be expressed in terms of Mach number according to the standard formula for adiabatic 1D expansion

$$\frac{A_e}{A_t} = \frac{1}{M}\left(\frac{1 + \frac{\gamma-1}{2}M^2}{\frac{\gamma+1}{2}}\right)^{\frac{\gamma+1}{2(\gamma-1)}}. \quad (29)$$

In order to cool gas flow down to the temperature, that is optimal for given carrier gas, one has to use nozzle specifically designed to the appropriate Mach number on the axis at the nozzle outlet. As well known, Mach number is related to temperature as follows:

$$T = \frac{T_0}{1 + \frac{\gamma-1}{2}M^2}. \quad (30)$$

Optimal gas flow pressure on nozzle outlet is assumed fixed to the same value for all considered gases $p_{tot} = 0.01$ torr. Optimal gas pressure in reservoir conditions can be obtained by the Poisson adiabat, Eq. (15), and optimal temperature in downstream gas flow temperature can be derived from calculations based on the Eerkens's model that are displayed in Fig. 1.

Let us introduce a new variable r in order to find relation between distance from the skimmer hole edge to the nearest cell border and cell characteristic dimensions. This variable is introduced as $r = \frac{v_{rest}}{v_{cell}}$, where $v_{rest} = v_{cell} - v_{flow}$ is the part of cell volume unoccupied by gas low. Gas flow volume can be estimated as $v_{flow} = \omega DHL$. By applying

formula (27) for cell volume, this distance takes the following form

$$\delta = -\frac{z}{4} + \frac{1}{4}\sqrt{z^2 + 4\omega HD\frac{r}{1-r}}, z = \omega D + H. \quad (31)$$

Equation (10) can be used to find relationship between dimensions of slit nozzle by combining it with Eq. (27) as follows:

$$\frac{D'H'}{DH} = \frac{k_B T_0 S \tau_p}{\Delta PL(1+\Gamma)}. \quad (32)$$

It can be rewritten as

$$\frac{k_B T_0 S \tau_p}{\Delta PL(1+\Gamma)} = \omega + 2\delta\left(\frac{\omega}{H} + \frac{1}{D}\right) + \frac{4\delta^2}{DH}. \quad (33)$$

By introducing a new variable $x = \frac{D}{H}$, this equation is reduced to the following

$$\frac{1}{2x}(\omega^2 - 1) + \left(\frac{3}{2} + \frac{r}{1-r}\right)\omega - \frac{1}{2} = \frac{k_B T_0 S \tau_p}{\Delta PL(1+\Gamma)}. \quad (34)$$

Therefore

$$x = \frac{\omega^2 - 1}{h_1 + h_2}, \ h_1 = 1 - \omega\left(3 + 2\frac{r}{1-r}\right),$$
$$h_2 = \frac{2k_B T_0 S \tau_p}{L_{\text{IC}} \Delta P(1+\Gamma)}. \quad (35)$$

On the other hand as follows from Eqs. (16, 24), nozzle throat area needed to produce a certain amount of isotopes M_{tot} by the end of enrichment operation t_f can be evaluated by

$$A_t = \frac{M_{\text{tot}}}{z_G(\aleph/n)N_{\text{nozz}}S(m_i/N_A)t_f}, \quad (36)$$

where m_i is boron-10 molar mass. Factor $z_G = v_B \tau_p$ takes into account gas flow intermittency caused by pulsed valve operation, where v_B is repetition rate of sequence of gas pulses. Number of pulses in each sequence is equal to number of recyclings n that is required in order to achieve desired enrichment level in gas portion emitted per pulse. Repetition rate of these sequences is $v_B = \frac{v}{n}$, where v is gas pulse repetition rate (apparently gas pulse repetition rate should coincide with laser pulse repetition rate). It can be also rewritten as

$$v_B = \frac{m}{t_f}. \quad (37)$$

Therefore, number of such gas pulse sequences produced over all enrichment operation time t_f is given by

$$m = \frac{t_f}{nt_c}. \quad (38)$$

Our next step in order to calculate IC volume is to find time necessary to evacuate gas from downstream cambers until required pressure level. By using Eqs. (12, 27, 35, 36) this time can be written as

$$t_{\text{out}} = \tau_p\left(\frac{x}{n\varepsilon} - 1\right) - t_{\text{tr}}, \ \kappa = \frac{D^2 t_f S(m_i/N_A)}{M_{\text{tot}}\mathcal{N}}, \ \varepsilon = \frac{1}{N_{\text{nozz}}\kappa}. \quad (39)$$

In these equations we introduced a new parameter that corresponds to global minimum of objective function

$$\mathcal{N} = \min_{\Omega}\{n/\aleph\} \quad (40)$$

over the set of parameters listed in the beginning of this section

$$\Omega = \{\text{CG}, \mu, \tau_p, r, D, L_{\text{IC}}, \Gamma, \bar{P}, T\}. \quad (41)$$

Number of nozzles N_{nozz} and laser pulse intensity I_P remain unknown. We find them from condition of minimality of total energy expenses and that pumpdown time should not be longer than gas molecule transition time across the IC $0 < t_{\text{out}} \le t_{\text{tr}}$. If gas molecule residence time is longer than this time, then it collides with walls and loses its excitation and selectivity deteriorates. Nonnegativeness condition of pumpdown time is also important because minimum of spent energy can be found at such IC volume, that this time gets negative. Apparently, the most efficient carrier gas should provide the lowest energy consumption and volume. As seen from Table 2, NO_2-carrier gas is the most energy efficient, while from the point of view of setup compactness using Ar is more advantageous.

Our results for optimal initial gas pressure in reservoir, downstream gas flow temperature for given carrier gas choice, and all other important parameters are summarized in Tables 1 and 2.

The second column of the last table from the right corresponds to the local minimum of the function, defined

Table 1 Optimal set of parameters for given carrier gas

CG	P_0, torr	T, K	D, μm	H, mm	L_{IC}, cm	L_{sk}, cm	r	τ_p, ms
N_2	82.954	23.736	10	15.7	20.6	2.57	0.73	19.28
Ar	7.66	22.95	100	38.1	125.6	13.8	0.95	91
NO_2	4.61	83.758	100	53.3	139	61	0.82	189.3
SF_6	3×10^{13}	12.22	10^{-12}	0.04	5×10^{-8}	5×10^{-10}	0.74	2726.2

Table 2 Optimal set of parameters for given carrier gas

CG	N_{nozz}	N_{in}	I_0,W	V_1,m^3	$\mathcal{N}$	E_{tot}, J
N$_2$	9.53×10^7	5.08×10^6	2.45×10^3	2.27×10^3	303.13	2.51×10^{13}
Ar	4.86×10^6	2.15×10^6	2.41×10^3	0.75×10^3	301.85	2.54×10^{13}
NO$_2$	8.15×10^6	3.94×10^6	942.2	1.02×10^4	294.5	1.755×10^{13}
SF$_6$	1.73×10^{23}	3.24×10^9	10.9	2.2×10^5	295.14	1.7315×10^{13}

by Eq. (40), that was evaluated by Optimization Toolbox subroutine 'NLPSolve' in Maple 15 [23]. We present our calculations of $\mathcal{N}$ as function of temperature for different carrier gases in Fig. 6a–d. It is seen that the smallest value of this function corresponds to NO$_2$-carrier gas.

By equating gas evacuation time defined by Eq. (39) to gas evacuation time defined by Eq. (12), one can deduce relationship between number of nozzles and number of vacuum pumps. It is seen that the value of latter is not necessarily an integer. This means that individual pumping speed should be adjusted. After substitution of Eq. (27) for IC volume into Eq. (12) the latter takes the next form

$$\Lambda = N_{in}g_0\rho v_{cell}(1+\Gamma), \;\; t_{out} = \Lambda\frac{N_{nozz}}{N_{in}}. \tag{42}$$

Thus the final relationship is the following

$$N_{in} = \Lambda\frac{N_{nozz}}{t_{out}}, \tag{43}$$

where t_{out} is given by Eq. (39). We calculated numbers of nozzles and vacuum pumps for different carrier gases, corresponding to annual production of 20 tons of enriched BCl$_3$, by this formula. Our results are shown in Table 2.

7 Summary

We introduced a new model for two-step iterative scheme of laser assisted isotope enrichment. The basic ingredient of this model is transport model proposed in [17]. This scheme can be represented as an iterative process, each stage of which corresponds to gas pulse emission followed by its irradiation, mechanical separation by skimmer blade, and pumping down. Isotopes are separated by selective action of the laser field on target molecules that triggers gas flow separation, caused by different diffusion rates of excited and non-excited (more heavier) species. We have argued that a static approximation can be applied for such scheme.

We compared two types of designs for industrial scale multipass cavities (IC), where gas flow is irradiated cross-wise. The first one corresponds to irradiation of the whole gas flow from one large throughput nozzle. The second one is when gas flow is divided into many sub-flows produced by relatively small nozzles that form rows parallel to each other. In this case more complete overlap between laser
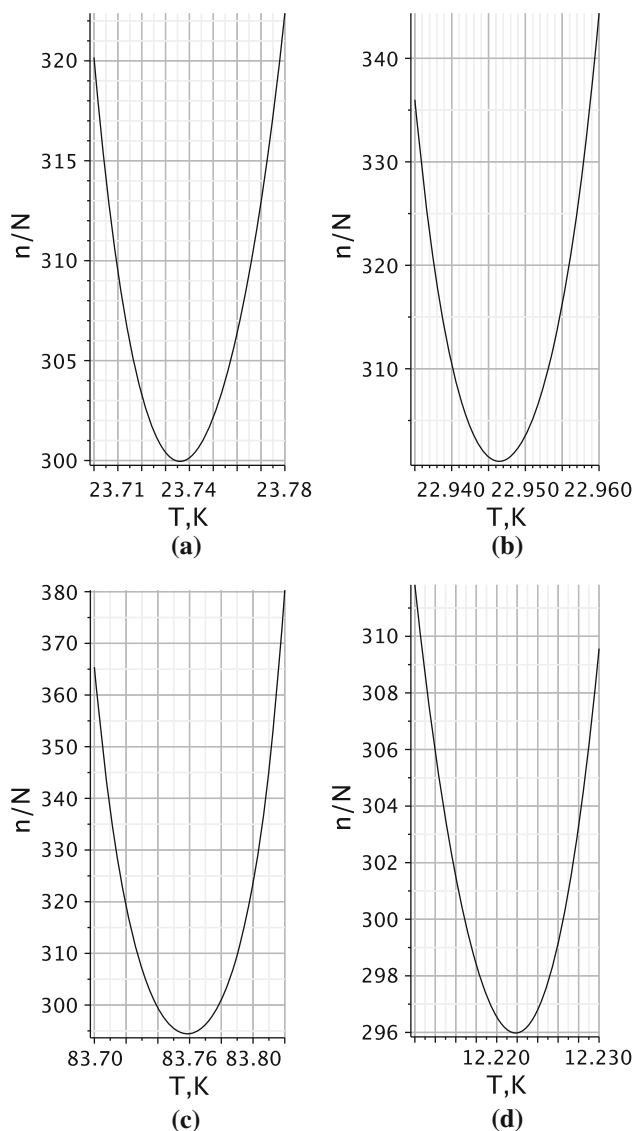

Fig. 6 Temperature dependence of an objective function $\mathcal{N}$ for **a** N$_2$, **b** Ar, **c** NO$_2$, and **d** SF$_6$ carrier gases. Corresponding optimal values of parameters are gathered in Table 1

beam and gas flows can be implemented by laser beam extension via its reflection from collection of mirrors installed on the opposite walls along gas flow direction. We have also demonstrated that enrichment performance of slit nozzle reduces dramatically with increase of its throat area. Therefore, only the last scheme should be considered.

We propose a general procedure to select optimal carrier gas, and calculate IC volume from the condition of minimum of energy spent to produce necessary amount of isotopes over given time interval, Eq. (25). The first task in order to satisfy this condition is to find optimal values of physical parameters that deliver global minimum of some objective function. This objective function is introduced as a number of iterations required for enrichment level to be achieved divided by recycling factor, Eq. (40). These physical parameters include carrier gas, valve opening time, nozzle throat height, IC length, skimmer chamber volume, distance between skimmer holes parameterized by factor r, temperature and pressure inside the gas flow. The minimal value of objective function after being found had been used to find downstream chambers pumpdown time, number of nozzles, number of vacuum pumps, and finally to find IC volume. It is also observed that NO_2 is the best carrier gas for boron isotope separation among others considered.

References

1. J.R. Lamarsh, *Introduction to Nuclear Engineering*, 2nd edn. (Addison-Wesley, 1983)
2. P.A. Bokhan, V.V. Buchanov, N.V. Fateev, M.M. Kalugin, M.A. Kazaryan, A.M. Prokhorov, D.E. Zakrevsky, *Laser Isotope Separation in Atomic Vapor* (WILEY-VCH Verlag GmbH & Co. KGaA, Weinheim, 2006)
3. A. Steigerwald et al., J. Appl. Phys. **112**, 013514 (2012)
4. P.F. Wang et al., J. Appl. Phys. **111**, 063517 (2012)
5. R.F. Barth, Appl. Rad. Isotopes **67**, S3–S6 (2009)
6. J.W. Eerkens, Nuclear Sci. Eng. **150**, 1–26 (2005)
7. V.N. Bagratashvili, V.S. Letokhov, A.A. Makarov, E.A. Ryabov, *Multiple Photon Infrared Laser Photophysics and Photochemistry* (OPA, Amsterdam, 1985)
8. J.W. Eerkens, Chem. Phys. **269**, 189–241 (2001)
9. J.W. Eerkens, Chem. Phys. Lett. **430**, 271–276 (2006)
10. N.V Karlov et al., ZhETF Pis. Red. **11**(4), 220–222 (1970)
11. J.W. Eerkens, *Rocket Radiation Handbook*, Vol. II. *Model Equations for Photon Emission Rates and Absorption Cross Sections*. (Air Research Manufacturing Company, 1973)
12. J.W. Eerkens, Laser Particle Beams **16**, 295–316 (1998)
13. J.M. Zellweger, Phys. Rev. Lett. **52**(7), 522–525 (1984)
14. H. Van den Bergh, Laser und Optoelectronik **3**, 263 (1985)
15. G. Herzberg, *Molecular spectra and Molecular Structure*. Vol. II (Krieger Publishing Company, Malabar, 1991)
16. J.W. Eerkens, Chem. Phys. **293**, 112–153 (2003)
17. J.W. Eerkens, Laser Particle Beams **23**, 225–253 (2005)
18. A.V. Arefiev, High Energy Density Phys. **6**, 121–127 (2010)
19. V.S. Letokhov, *Laser Control of Atoms and Molecules* (Oxford University Press, New York, 2007)
20. G.W.F. Drake (ed.) *Handbook of Atomic, Molecular, and Optical Physics* (Springer, Berlin, 2006)
21. R. Courant, K.O. Friedrichs, *Supersonic Flow and Shock Waves* (Interscience Publishers, Inc., New York, 1956)
22. M. Kumar, V. Gupta, A.K. Nath, Appl. Phys. B **80**, 757–763 (2005)
23. Maple 15: http://www.maplesoft.com
24. D.M. Hoffman, *Handbook of Vacuum Science and Technology* (Academic Press, New York, 1998)